Second-order Zeeman effect in the $5\,^2S-3\,^2S$ and $4\,^2D-3\,^2S$ two-photon transitions of atomic sodium

W. Hüttner, P. Otto, and M. Gamperling
Abteilung Chemische Physik, Universität Ulm, D-89069 Ulm, Germany
(Received 14 March 1996)

We have observed the second-order, field-induced Zeeman effects of the Doppler-free two-photon transitions $5\,^2S-3\,^2S$ and $4\,^2D-3\,^2S$ of atomic sodium using fields up to 5 T. Using a suitable experimental configuration it was possible to avoid the appearance of first-order effects in the high-field limit. The remaining small field-induced shifts are of the order of magnitude of a few linewidths. They yield the differences of the diamagnetic susceptibilities of the connected atomic states. The method is therefore capable of providing data related to atomic electronic structure. [S1050-2947(96)01508-9]

PACS number(s): 32.60.+i, 32.10.Dk

I. INTRODUCTION

Diamagnetism, manifest as repulsive field-induced forces, is a common property of all kinds of ordinary matter. It is caused by the Larmor precession of the electrons around the field axis, and the oppositely directed, associated magnetic moments. Diamagnetic interactions are comparably weak, and masked by strong attractive forces when spin or orbital paramagnetism is present as in most atomic states. The quantum-mechanical diamagnetic energy in a field $\mathbf{B}=(0,0,B)$ is given by Van Vleck's [1] expression

$$\hat{H}^{(2)}=\frac{e^2}{8m}\sum_i (x_i^2+y_i^2)B^2=\frac{e^2}{8m}\sum_i r_i^2 \sin^2\vartheta_i B^2, \quad (1)$$

where (x_i,y_i,z_i) is the radius vector of length r_i of the ith electron and ϑ_i its polar angle. m and e are the electron's mass and the magnitude of its charge, respectively. In an atom with the nucleus as the natural origin the isotropic susceptibility is defined by

$$\xi=-\frac{e^2}{6m}\left\langle \sum_i r_i^2 \right\rangle, \quad (2)$$

where the brackets mean the expectation value over the function diagonalizing the total Hamiltonian of the system (in molecules the Larmor precession is partly quenched, leading to positive tensorial corrections [1]).

ξ, as defined in Eq. (2), is a basic atomic quantity related to electronic structure and changing with electronic state. It is therefore surprising that so few values are known. The ground-state susceptibilities of the inert gases have been measured by the classical Gouy balance method [2], and that of neon has also been derived from electron diffraction results [3]. A large body of literature deals with *ab initio* calculations and special Thomas-Fermi computations of ξ in the atomic ground state [4,5] where the underlying theoretical concepts are currently under discussion [6]. Spectroscopic data are available from Rydberg states of hydrogen [7], the alkali-metal atoms [8,9], and nonhydrogenlike systems [10,11]. It is evident from $\hat{H}^{(2)}$ that high excitation leads to strong second-order Zeeman effects. Miller and Freund [12] have drawn susceptibility information for the $4\,^3P$ state of helium from a microwave-optical double resonance experiment.

The purpose of the present paper is to show that suitable experimental conditions can be chosen to resolve the field-induced Zeeman effects in atomic levels close to and including the ground state. The linear Zeeman effects can be suppressed and do not have to be included in the analysis. The spectra yield the differences of susceptibilities of the levels connected by the spectroscopic transitions. As a first example, we give the results for ^{23}Na in the states addressed in the title.

II. THEORETICAL BACKGROUND

We treat sodium in the usual way as a hydrogenic atom consisting of the shielded nucleus (core) and the valence electron. The effective Hamiltonian reads

$$\hat{H}=\hat{H}_0+\hat{H}_{\mathrm{FS}}+\hat{H}_{\mathrm{HFS}}-g_l\mu_B\hat{L}_z B-g_s\mu_B\hat{S}_z B-g_I\mu_B\hat{I}_z B$$
$$-\tfrac{1}{2}\hat{\boldsymbol{\xi}}(n,l)B^2\tfrac{3}{2}\sin^2(\mathbf{r},\mathbf{B})-\tfrac{1}{2}\hat{\boldsymbol{\xi}}(\mathrm{core})B^2, \quad (3)$$

where $\hat{H}_0$ means the zero-field Hamiltonian excluding fine (FS) and hyperfine (HFS) interactions. $\hat{L}_z$, $\hat{S}_z$, and $\hat{I}_z$ are the orbital, electron spin, and nuclear spin angular momentum components along the field axis z; g_l, g_s, and g_I are the (negatively chosen) orbital and electron spin g values and the nuclear g value, respectively, with their corresponding moments expressed in units of the Bohr magneton μ_B. The operator

$$\hat{\xi}(n,l)=-\frac{e^2}{6m}r^2, \quad (4)$$

defined in accordance with Eqs. (1) and (2), refers to the susceptibility of the valence electron having nuclear distance r in the state (n,l), and $\hat{\xi}$(core) to that of all other electrons. For large fields, the energy can be written in the high-field limit because interstate perturbations are negligible in the low quantum states considered here. This leads, in sufficient accuracy for the levels involved, to

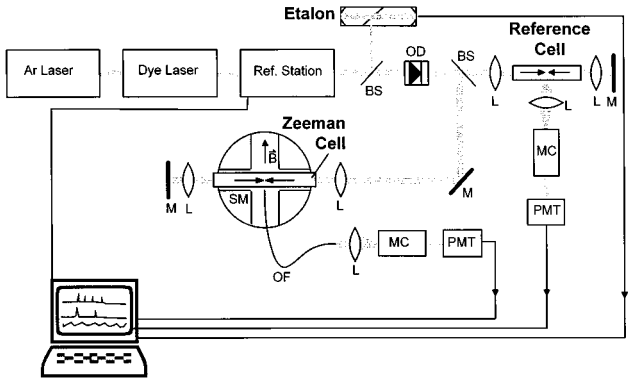

FIG. 1. Apparatus used for the experiments. BS, beam splitter; L, collimating lens; M, plane mirror; MC, monochromator; PMT, photomultiplier tube; OD, optical diode; SM, superconducting magnet; $\vec{B}$, magnetic field. The fluorescence resulting from the Doppler-free two-photon excitation is collected longitudinally to the field and guided into the amplification channel by an optical fiber (OF). In Figs. 2 and 3 parallel recordings of the Zeeman, reference, and étalon traces are shown as functions of the laser frequency.

$$E=E_{nl}^{0}+(\mathrm{FS})_{nls}m_l m_s+(\mathrm{HFS})_{nsI}m_s m_I-g_l\mu_B m_l B-g_s\mu_B m_s B-g_I\mu_B m_I B-\frac{1}{2}\,\xi(n,l)B^2 3\frac{l(l+1)+m_l^2-1}{(2l-1)(2l+3)}-\frac{1}{2}\,\xi(\mathrm{core})B^2, \quad (5)$$

where

$$\xi(n,l)=-\frac{e^2}{6m}\langle n,l|r^2|n,l\rangle. \quad (6)$$

In the following, we specify $m_l=0$ and the transition selection rules $\Delta m_s=\Delta m_l=\Delta m_I=0$. It is seen from Eq. (5) that the fine-structure term vanishes under these circumstances, and that the lower and upper atomic states show identical first-order field effects which thus cancel in the Zeeman spectrum. As the sodium nucleus has spin $\frac{3}{2}$ we expect the four equidistant components labeled $m_s m_I=-\frac{3}{4}$, $-\frac{1}{4}$, $\frac{1}{4}$, $\frac{3}{4}$ which are all subject to identical quadratic field shifts [last line in Eq. (5)].

III. EXPERIMENT

Experimental setup and field as well as light propagation configurations are shown in Fig. 1. Fields up to 5 T are provided in a superconducting Oxford Instruments magnet. The Doppler-free two-photon transitions are observed recording the intensity of the cascade fluorescence $3\,^2P-3\,^2S$ channel via a monochromator. The field shifts were measured simultaneously relative to suitably chosen HFS zero-field components using a confocal étalon [free spectral range (FSR) equal to (193.6±0.6) MHz], calibrated against the well-known doublet splitting of (1616.4±1.4) MHz of the $5\,^2S-3\,^2S$ transition of sodium [13,14]. A Spectra Physics ring dye laser was employed, using powers of approximately 500 mW for the Zeeman and 30 mW for the zero-field spectra. Linewidths achieved were approximately 13 MHz on the atomic scale which is twice the laser frequency scale.

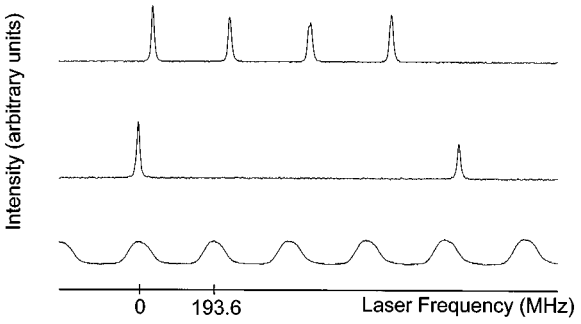

FIG. 2. Zeeman pattern of the Doppler-free $5\,^2S-3\,^2S$ two-photon transition of sodium at $B=4.64$ T. The first member of the quartet (upper trace) is the magic doublet. It is frequency displaced from the $F=2$ zero-field component (left signal in the second trace) because the atomic susceptibilities of the two participating states are different. The third trace shows the transmission signal of the étalon used for frequency measurement [FSR equal to (193.6±0.6) MHz].

The Paschen-Back limit selection rules of $S\leftarrow S$ two-photon transitions are $\Delta m_s=\Delta m_I=0$ irrespective of polarization and propagation of the laser light relative to the field [15], those of $D\leftarrow S$ transitions read $\Delta m_s=\Delta m_I=0$ and $\Delta m_l\leqslant 2$ [16]. $\Delta m_l=0$ as required here can be realized either by choosing the same direction of linear polarization for both beams (as has been done in our experiments), or by using equally sensed circular polarization in the longitudinal field configuration. Our laser beams are directed perpendicularly to the magnetic field, and we detect the fluorescence intensity in direction of the field. The signal is maximal when the polarization of the laser light is chosen perpendicular to **B**, i.e., perpendicular to the drawing plane of Fig. 1.

IV. RESULTS AND DISCUSSION

Figure 2 shows the high-field quartet of the $5S$-$3S$ transition at fields near 4 T. The first (low-frequency) member of the quartet, $F'_{\max}$-$F_{\max}$=2-2, $\pm(m_F)'_{\max}$-$\pm(m_F)_{\max}$=±2-±2 is the coalescing magic doublet not subject to decoupling effects at any field strength (compare Fig. 1 of Ref. [15]). Its frequency shift $\Delta\nu=\Delta\nu(B)$, relative to the $F=2$ zero-field position, is therefore caused solely by the second-order Zeeman effect [last line in Eq. (5), $l=0$]. A plot of $\Delta\nu$ versus B^2 is given in the upper part of Fig. 4. The slope of the straight line, obtained in a least squares fit as $\Delta\nu/B^2=(4.51\pm0.12)$ MHz T^{-2} on the atomic scale, is a direct measure of the quantity $\xi(5,0)$-$\xi(3,0)$ of the sodium atom.

Biraben, Cagnac, and Grynberg [16] have observed the Paschen-Back effect of the $4\,^2D-3\,^2S$, $\Delta m_l=2$ Doppler-free two-photon transition using fields up to 0.97 T. They have seen an octet because of the doublet fine structure of the $m_l=2$ D level. As explained above we have chosen the $m_l=0$, $\Delta m_l=0$ group of lines in order to avoid first-order Zeeman shifts owing to orbital magnetism. It develops, as predicted, also into an equally spaced quartet of lines as shown in Fig. 3. The high-field limit is reached at 2.5 T

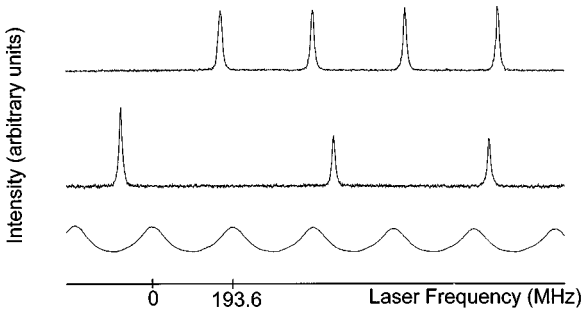

FIG. 3. High-field pattern of the Doppler-free $4\,^2D-3\,^2S$ two-photon transition at $B=4.90$ T. The frequency shifts of the fourth member of the $m_l=\Delta m_l=0$ quartet (upper trace) were measured against the third zero-field component at different fields starting at 0.5 T (the fourth zero-field component appearing at higher frequency cannot be seen here).

beyond which only second-order shifts of the quartet are seen. We have verified that all four lines show the same effect within our experimental accuracy. The shifts $\Delta\nu$ of the last quartet member (highest frequency) were measured using the third zero-field component as reference. They are plotted as a function of B^2 in the lower part of Fig. 4. The slope is $\Delta\nu/B^2=(3.37\pm0.17)$ MHz T^{-2} on the atomic scale.

The two results stand, of course, independent of the special formulation of the second-order Zeeman Hamiltonian of sodium in Eq. (3). A convenient test of the core-plus-valence electron model is possible on grounds of the well-known expression

$$\langle n,l|r^2|n,l\rangle=\frac{n^2}{6Z^2}\,(15n^2-9l^2-9l+3)a_0^2, \qquad (7)$$

valid for hydrogen and one-electron ions of nuclear charge Ze (a_0 is the Bohr radius). With Eq. (6), $Z=1$, and replacing n by $n^*=n-\Delta(n,l)$, and l by $l^*=l-\Delta(n,l)$ where $\Delta(n,l)$ are the accepted empirical quantum defects of sodium [17] we calculate the isotropic susceptibilities, given in the fourth column of Table I, which by definition do not contain the core contribution. Using these values of $\xi(n,l)$ in Eq. (5) we obtain the values of $\Delta\nu/B^2$ given in the third column of Table II which compare unexpectedly well with the experimental results repeated in the last column. The agreement is less good for $l=0$ as expected for a penetrating orbit. Note that subtracting $\Delta(n,l)$ from both n and l ensures that the number of radial nodes remains constant in comparison with the true one-electron atom. Replacing only n by n^* and leaving l unchanged in Eq. (7) as earlier suggested by Van Vleck [1] leads to the slightly different predictions in the third column of Table I and in the second column of Table II, respectively. Subtracting $\xi(3,0)$ from a Hartree-Fock result for the ground state [4] we calculate $\xi(\text{core})=-0.135\times10^{-27}$ J T^{-2} which is a small contribution as compared with those of the valence electron in the last column of Table I. The results of the simple analysis based on the one-electron model of sodium gives confidence in the validity of evaluating the experimental data in terms of the high-field energy expression Eq. (5). A comparison with accurate literature *ab initio* results is not possible yet.

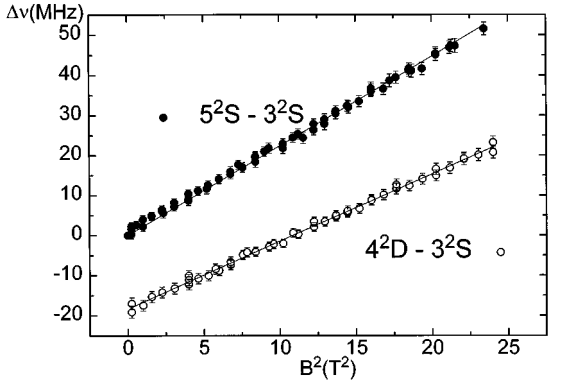

FIG. 4. The field-induced frequency shifts of the indicated transitions as a function of the squared field strength. Linear least squares fits result in the slopes $\Delta\nu/B^2$ given in the last column of Table II.

TABLE I. Calculated valence electron susceptibilities $\xi(n,l)$. The first column shows the quantum numbers of the involved states; the second their quantum defects $\Delta(n,l)$. In the third column $\xi(n,l)$ is calculated as described in Eq. (6) using $n^*=n-\Delta(n,l)$ for n; in the fourth column l is additionally replaced by $l^*=l-\Delta(n,l)$.

		$\xi(n,l)$ (10^{-27} J T^{-2})	
(n,l)	$\Delta(n,l)$	(n^*,l)	(n^*,l^*)
(3,0)	1.373	−0.248	−0.221
(5,0)	1.352	−5.910	−5.786
(4,2)	0.011	−6.546	−6.563

V. CONCLUSION

In conclusion, we have resolved the second-order Zeeman effect in low-lying quantum states of an alkali-metal atom. The experimental accuracy could be improved using an étalon of better finesse and shorter FSR for frequency interpolation. The method can also be useful for other more interesting atoms than sodium. In genuine many-electron cases such as the noble-gas atoms the anisotropic susceptibility term should be included explicitly in the analysis of the field shifts for states $l>0$ [12]. Possible applications of accurate atomic susceptibilities are the measurements of strong labo-

TABLE II. The measured second-order Zeeman effects in comparison with predictions using the one-electron susceptibilities in Table I.

	$\Delta\nu/B^2$ (MHz T^{-2})		
	Calc.		Expt.[a]
Transition	(n^*,l)	(n^*,l^*)	
$5\,^2S-3\,^2S$	4.27	4.20	4.51(12)
$4\,^2D-3\,^2S$	3.34	3.37	3.37(17)

[a]The uncertainties in parentheses in units of the least significant figure are three standard deviations of the least squares fits.

ratory fields and, of course, tests of wave functions. A teslameter using second-order Zeeman effects of the kind discussed here would especially be insensitive against inhomogeneities in comparison with methods based on first-order effects.

ACKNOWLEDGMENTS

The support of the Deutsche Forschungsgemeinschaft and of Fonds der Chemischen Industrie are gratefully acknowledged.

[1] J. H. Van Vleck, *Theory of Electric and Magnetic Susceptibilities* (Oxford University Press, New York, 1932).
[2] C. Barter, R. G. Meisenheimer, and D. P. Stevenson, J. Phys. Chem. **64**, 1312 (1960).
[3] Y. Zhang and M. Fink, Phys. Rev. A **35**, 1943 (1987).
[4] L. B. Mendelsohn, F. Biggs, and J. B. Mann, Phys. Rev. A **2**, 1130 (1970).
[5] B. G. Englert and J. Schwinger, Phys. Rev. A **29**, 2353 (1984).
[6] M. Levy and J. P. Perdew, Phys. Rev. A **32**, 2010 (1985).
[7] P. A. Braun, Rev. Mod. Phys. **65**, 115 (1993).
[8] F. A. Jenkins and E. Segrè, Phys. Rev. **55**, 52 (1939).
[9] C. D. Harper and M. D. Levenson, Opt. Commun. **20**, 107 (1977).
[10] W. R. S. Garton and F. S. Tomkins, Astrophys. J. **158**, 839 (1968).
[11] P. F. O'Mahony and K. T. Taylor, Phys. Rev. Lett. **23**, 2931 (1986).
[12] T. A. Miller and R. S. Freund, Phys. Rev. A **4**, 81 (1971).
[13] P. Tsekeris, K. H. Liao, and R. Gupta, Phys. Rev. B **13**, 2709 (1976).
[14] G. Grynberg and B. Cagnac, Rep. Prog. Phys. **40**, 791 (1977).
[15] N. Bloembergen, M. D. Levenson, and M. M. Salour, Phys. Rev. Lett. **32**, 867 (1974).
[16] F. Biraben, B. Cagnac, and N. Grynberg, Phys. Lett. **48A**, 469 (1974).
[17] F. K. Richtmeyer, E. H. Kennard, and T. Lauritsen, *Introduction to Modern Physics* (McGraw-Hill, New York, 1956).